ELSEVIER

Thermochimica Acta 335 (1999) 27–42

thermochimica acta

www.elsevier.com/locate/tca

Aging of polycarbonate studied by temperature modulated differential scanning calorimetry

John M. Hutchinson*, Ang Boon Tong, Zhong Jiang

Department of Engineering, King's College, University of Aberdeen, Aberdeen AB24 3UE, UK

Received 7 December 1998; accepted 20 May 1999

Abstract

The enthalpy relaxation behaviour of polycarbonate has been studied by alternating differential scanning calorimetry (ADSC). Samples have been annealed at 125°C, about 20°C below their glass transition temperature, for periods up to 2000 h, and then scanned in the ADSC using the modulation conditions: heating rate=1 K min^{-1}; temperature amplitude=1 K; period=1 min. The data have been analysed in terms of total, reversing and non-reversing heat flows, and also in terms of complex, in-phase and out-of-phase specific heat capacities and a phase angle. The effect of aging time on each of these parameters is illustrated and compared with the predictions of an earlier theoretical model. It is shown that there is very good agreement between the experimental results and the theoretical predictions, the most important aspects being the following. The total heat flow closely corresponds to conventional DSC in respect of both peak endotherm temperature and enthalpy loss (derived from the area under the peak). In contrast, the non-reversing heat flow peak area does not provide a good measure of the enthalpy loss because the reversing heat flow (and complex specific heat capacity) depends significantly on aging, the transition region becoming much sharper as the aging time increases. Likewise, the phase angle (when appropriately corrected for the problem of heat transfer) also becomes sharper on aging, and the (negative) peak moves towards higher temperatures. The out-of-phase specific heat capacity is calculated using the corrected phase angle, and it is shown that the area under this peak is essentially independent of aging time, confirming another prediction from the earlier theoretical model that this area provides no information about the enthalpy loss that occurs during the aging process.

Keywords: Polycarbonate; Temperature modulated differential scanning calorimetry; Alternating differential scanning calorimetry; Enthalpy relaxation; Aging

1. Introduction

In the five years or so since the original conception by Reading [1] of the idea of temperature modulated differential scanning calorimetry (TMDSC) and since its commercialisation in various forms (modulated DSC, MDSC, TA Instruments; Alternating DSC, ADSC, Mettler-Toledo; Dynamic DSC, DDSC, Perkin-Elmer), TMDSC has seen an exponential growth in interest. Much of this has been fuelled by a desire to find new applications and advantages for this exciting new thermal analytical technique. In some areas, such as the separation of overlapping transitions of a different nature in polymer blends [1,2] and the monitoring of the degree of cure during the crosslinking reaction of thermosetting polymers, [3,4] the advan-

*Corresponding author. Tel.: +44-1224-272791; fax: +44-1224-272497

E-mail address: j.m.hutchinson@eng.abdn.ac.uk (J.M. Hutchinson)

0040-6031/99/$ – see front matter
PII: S0040-6031(99)00134-3

tages of TMDSC over conventional DSC have been clearly demonstrated. In other areas, for example, its application to first order transitions such as crystallisation and melting, these advantages are less obvious in view of the continued debate about the interpretation of various aspects of the TMDSC response.

In contrast to the latter examples, the application of TMDSC to the glass transition of polymers (or of any glass forming system in general) provides a good illustration of how the TMDSC response can be interpreted well through the use of a model for the behaviour of the sample when subjected to the temperature modulations superimposed on the constant heating (or cooling) rate. For example, in earlier work we made use of a simple kinetic model, successfully applied in the interpretation of conventional DSC data, to describe semi-quantitatively all of the important characteristic features manifest by TMDSC for polymers in the glass transition region [5,6]. These features may be summarised as follows for a typical TMDSC heating scan:

1. a sigmoidal change in complex and in-phase specific heat capacities, C_p^* and C_p', respectively, from glassy to liquid state values;
2. the temperature T_{mid} at which the mid-point of the above sigmoidal change occurs, sometimes referred to as a dynamic glass transition, increases with increasing frequency of the modulation;
3. the phase angle ϕ and the out-of-phase specific heat capacity C_p'' are both negative in the transition region (indicating that the heat flow lags behind the heating rate), their negative values passing through a maximum at a temperature approximately equal to T_{mid};
4. the average heat flow response is very similar to that which would be observed by conventional DSC at the same underlying heating rate.

A subsequent more quantitative application of the same simple kinetic model [7] predicted the TMDSC response of glassy polymers which have been annealed (or aged) at a temperature closely below their glass transition temperature. These predictions may be summarised as follows:

1. the sigmoidal change in C_p^* and C_p' becomes sharper, and T_{mid} increases slightly, as the aging time increases;
2. the peaks in the phase angle ϕ and in C_p'' become sharper as the aging time increases, but the area under the C_p'' peak remains constant;
3. the average specific heat capacity, $C_{p,\mathrm{ave}}$, derived from the average heat flow, closely follows the specific heat capacity that would be obtained by conventional DSC at the underlying heating rate;
4. the area under the $C_{p,\mathrm{ave}}$ curve, relative to the $C_{p,\mathrm{ave}}$ curve for an unannealed sample, gives the enthalpy lost during aging.

The extent to which these predictions are borne out in practice is examined in detail in the present paper, with reference to ADSC experiments on samples of polycarbonate annealed about 20°C below its glass transition temperature ($T_g \approx 145$°C).

2. Experimental and materials

The material used for this study was a commercial grade of polycarbonate of bisphenol-A (Tecanat, Ensinger), provided in the form of solid extruded rod about 40 mm diameter. A length of this extruded rod was cut axially into four equal quadrants, and from the central part of each quadrant a rod of 5 mm diameter was turned on a lathe. From these rods, disc specimens of approximately 0.5 mm thickness were pared off on a lathe using a sharp paring tool. This provided many specimens, suitable for placing within standard aluminium pans used in the Mettler-Toledo ADSC, all with a mass of approximately 12 mg and all with the same good surface finish (which is important in respect of the heat transfer characteristics between instrument and sample).

Before any aging experiment, the samples were heated at 20 K min^{-1} in the ADSC to a temperature of 180°C, about 35°C above T_g, in order to erase their previous thermal history. They were then cooled at a controlled rate of 10 K min^{-1} to the aging temperature of 125°C. Samples which were to be aged for a period of 4 h or less were left in the ADSC at 125°C to age in situ. All the other samples, with aging times greater than 4 h, were removed from the ADSC when the temperature of 125°C was reached, and were placed on an aluminium block in a temperature-controlled oven, previously set at 125°±0.5°C. The aluminium

block was drilled with a 7 × 7 array of shallow holes of diameter and depth suitable for accepting the polycarbonate samples. The location, date and time of entry of each sample into the oven allowed multiple samples to be used with known aging times ranging up to about 2000 h. The temperature of the aluminium block was monitored constantly using a copper–constantan thermocouple. At the appropriate aging time as required (at approximately equal intervals of logarithmic time), samples were removed from the oven and transferred to the ADSC for scanning through the glass transition region.

The instrument used was a Mettler-Toledo ADSC with STAR^e software, version 5.11, and was equipped with an intracooler and automatic sample handling. Temperature calibration was performed with indium and the purge gas was dry nitrogen at a controlled flow rate. The temperature programme selected was the so-called 1,1,1 combination, for which the underlying heating rate is 1 K min^{-1}, the temperature amplitude is 1 K and the period is 1 min, and the temperature range covered was from 80°C to 180°C.

Prior to scanning an annealed sample, it was necessary to perform ''empty'' and ''blank'' runs as part of the ADSC calibration procedure. For the empty run, a 1,1,1 scan was made over the full temperature range of 80–180°C with nothing in either the sample or reference side of the ADSC cell; this allows for corrections for any asymmetry of the cell. For the blank run, a 1,1,1 scan was again made over the full temperature range, this time with an aluminium pan on the reference side and an aluminium pan plus lid on the sample side; this allows for calibration of the heat flow from known values of the specific heat capacity for aluminium and from the measured difference in mass of aluminium between sample and reference side (approximately the mass of the lid). Finally, the sample run can be made, using the same pans and lid that have been used for the calibration.

To scan an aged sample in the ADSC, the required sample is transferred from the oven at 125°C (for samples with aging times greater than 4 h, otherwise the sample is already in the ADSC) into the ADSC at 125°C, cooled at 10 K min^{-1} to 80°C, and then scanned from 80°C to 180°C using the 1,1,1 programme. When this run was complete, the sample could be cooled again at 10 K min^{-1} to 125°C and then used again for another aging time.

3. Data analysis

The data analysis procedures are best described by reference to typical output from the ADSC. Fig. 1 shows the modulated heat flow signal for a sample scan after only a short annealing period (0.1 h) at 125°C. The transition from the glassy state at low temperatures to the liquid-like state at high temperatures is clearly visible from the change in amplitude of the modulations. Less clear, but visible on closer inspection, is a change in the average value of the modulations, which also includes a small endothermic (downwards in Fig. 1) overshoot.

By ''clicking'' on the sample, blank and empty curves simultaneously, the latter two having previously been obtained from the calibration procedure, the STAR^e software ADSC routine performs the Fourier transformation from which the average value and amplitude of the heat flow signal are obtained, together with a phase angle, ϕ. These are then used to evaluate a number of output quantities, which can be classified according to two types of analysis.

The first approach is to define a complex specific heat capacity, the modulus of which is given by

$$C_p^* = \frac{A_{\mathrm{HF}}}{A_{\mathrm{q}}}, \tag{1}$$

where A_{HF} and A_{q} are the amplitudes of the heat flow and heating rate, respectively. This can be separated into in-phase (C_p') and out-of-phase (C_p') components using the phase angle ϕ between heat flow and heating rate:

$$C_p' = C_p^* \cos\phi, \tag{2}$$

$$C_p' = C_p^* \sin\phi. \tag{3}$$

The second approach is to consider so-called reversing and non-reversing effects. The total heat flow is given by the average value from the Fourier transformation. The reversing heat flow is found as the heat flow amplitude, A_{HF}, scaled to the underlying heating rate. The non-reversing heat flow is then defined simply as the total heat flow minus the reversing heat flow.

Fig. 2 shows the result of such a transformation procedure on the data shown in Fig. 1, with the upper four curves relating to the first type of analysis (complex specific heat capacity) and the lower three curves

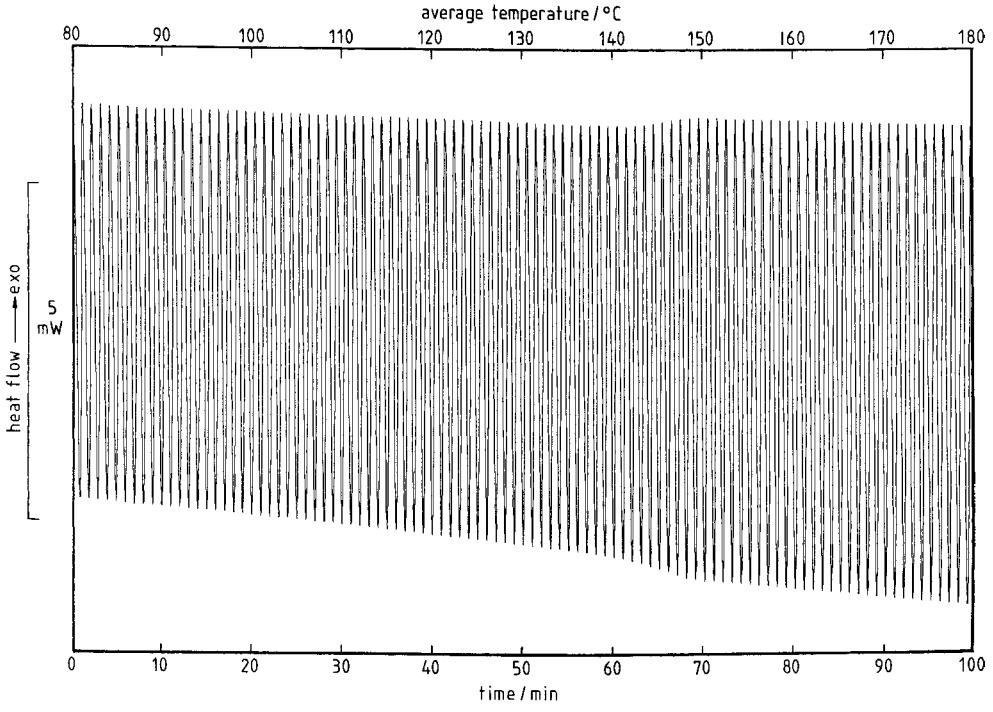

Fig. 1. Modulated heat flow versus time (lower scale) and average temperature (upper scale) for a polycarbonate sample aged for 0.1 h at 125°C. Underlying heating rate=1 K min^{-1}, amplitude of temperature modulation=1 K, and period of modulation=1 min. The exothermic heat flow direction is upwards.

relating to the second type (reversing and non-reversing heat flows). A number of characteristic features can be seen from these curves, including sigmoidal changes in C_p^* and C_p', peaks (and step changes, see below) in C_p' and ϕ, a peak and a step change in the total heat flow, a sigmoidal change in the reversing heat flow, and a peak in the non-reversing heat flow. All of these features are anticipated theoretically [5–7], and will be examined further below; first, though, one particular detail requires closer attention.

Well below and well above the glass transition region, the phase angle ϕ (and hence also C_p') is anticipated to be zero. Although not shown in Fig. 2, because a relative rather than absolute scale is used for the phase angle, ϕ is not zero in either the glassy or liquid-like regions, but instead displays a certain negative value. Furthermore, the non-zero value for ϕ is different in the glassy and liquid-like regions, which is the cause of the step changes in ϕ and C_p'' (in addition to the peaks) mentioned above. This effect is universally observed, and the origin is the problem of heat transfer. A correction procedure, originally suggested by Schick and co-workers [8] and demonstrated by Jiang et al. [9,10], has been incorporated into the Mettler-Toledo STAR^e software, and has been used throughout the present work to obtain corrected phase angles and corrected C_p'' values.

With the above considerations in mind, the characteristic features of the transformed ADSC curves can be quantified by a number of parameters defined with reference to the schematic illustration in Fig. 3. The sigmoidal complex specific heat capacity curve is quantified by a width W, defined as the temperature difference between an onset (intersection of extrapolated glassy line and inflexional tangent) and endset (intersection of extrapolated liquid line and inflexional tangent) of the specific heat capacity change, and by a mid-point temperature T_{mid}, where the curve passes mid-way between the extrapolated liquid and glassy lines. The corrected phase angle is quantified by the temperature $T_{max}(\phi)$ at which the maximum departure occurs, by the magnitude of this maximum departure $\Delta\phi_{max}$, and by the half-width of the peak $W_{1/2}$.

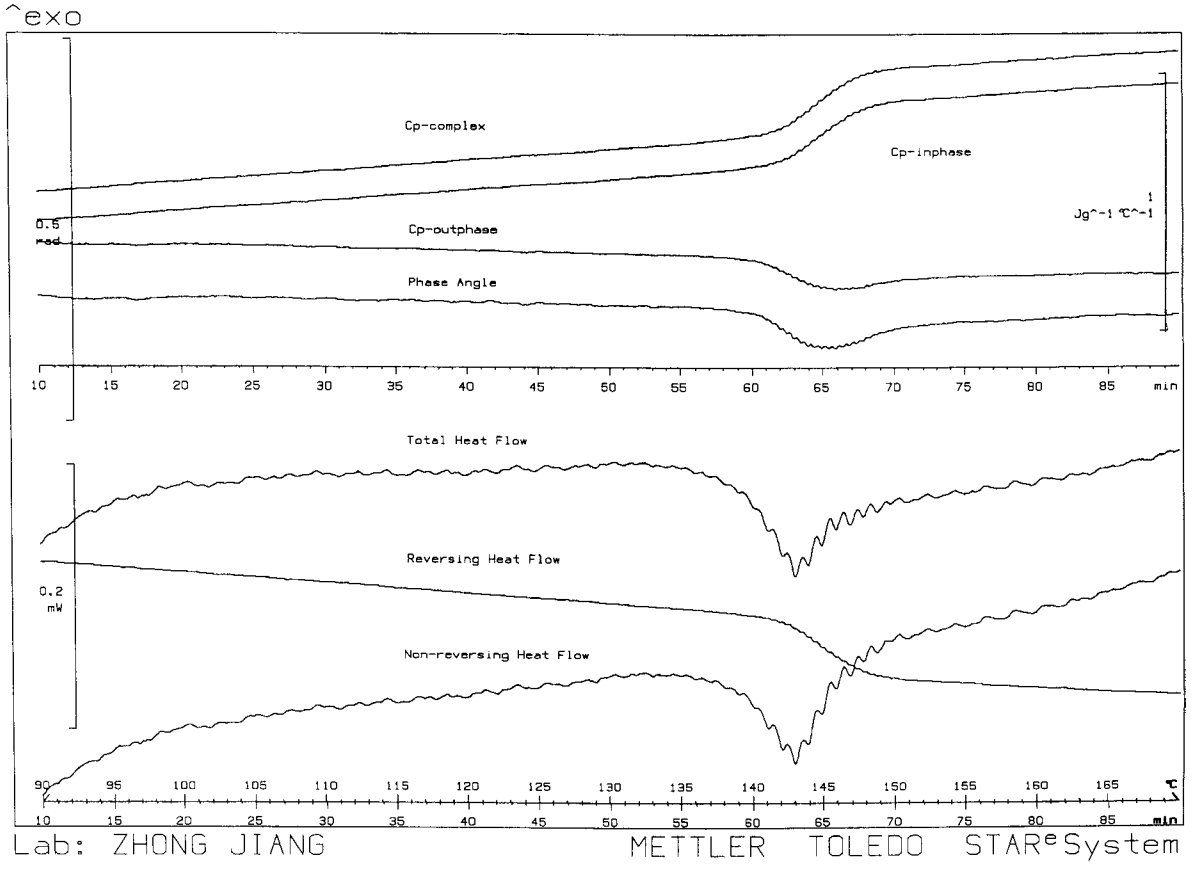

Fig. 2. ADSC transformed curves for the heat flow modulations shown in Fig. 1. The upper four curves relate to the complex specific heat capacity approach: the scale bar for specific heat capacity is shown to the right; that for the phase angle is shown to the left. The lower three curves show the total, reversing and non-reversing heat flows, with the scale bar shown to the left. Note that all these scales are relative, and that curves have been shifted vertically for clarity. The exothermic heat flow direction is upwards.

All of these quantities, defined with reference to Fig. 3, together with some others to be defined further below, will be used to show how the ADSC response of glassy polycarbonate is influenced by the effect of aging at T_g-20 K.

4. Results

Fig. 4 shows a family of curves for the total heat flow as a function of time (or temperature) for samples annealed at 125°C for times between 1 and 2000 h. The overall effect of aging is clear: there is a sigmoidal step change in heat flow upon which is superimposed an endothermic peak, which grows in magnitude and moves to higher temperature as the aging time increases. This is a well-known effect (e.g., see [11,12]) displayed in conventional DSC scans of aged polymers, even if it is more usual for these curves to be shown endothermic upwards.

When the reversing heat flow (which is simply a scaled and inverted copy of the complex specific heat capacity, shown further below) is subtracted from the total heat flow, the non-reversing heat flow is obtained. This is shown in Fig. 5. Here again the overall effect of aging is clear: an endothermic peak increases in magnitude and shifts to higher temperatures as the aging time increases. In contrast to the total heat flow, the non-reversing heat flow does not display any sigmoidal step change on going from the glass to

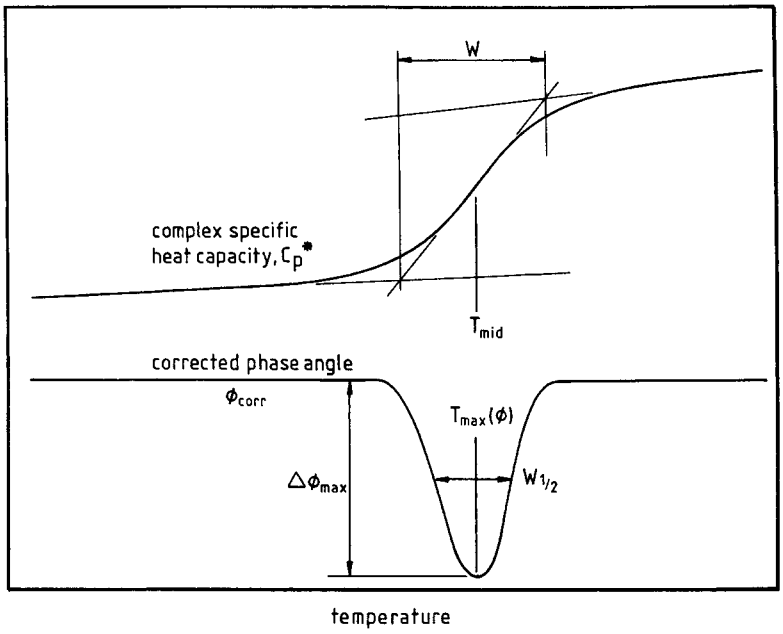

Fig. 3. Schematic illustration of the complex specific heat capacity C_p^* and corrected phase angle ϕ_{corr} curves as a function of temperature, showing how various characteristic quantities are defined.

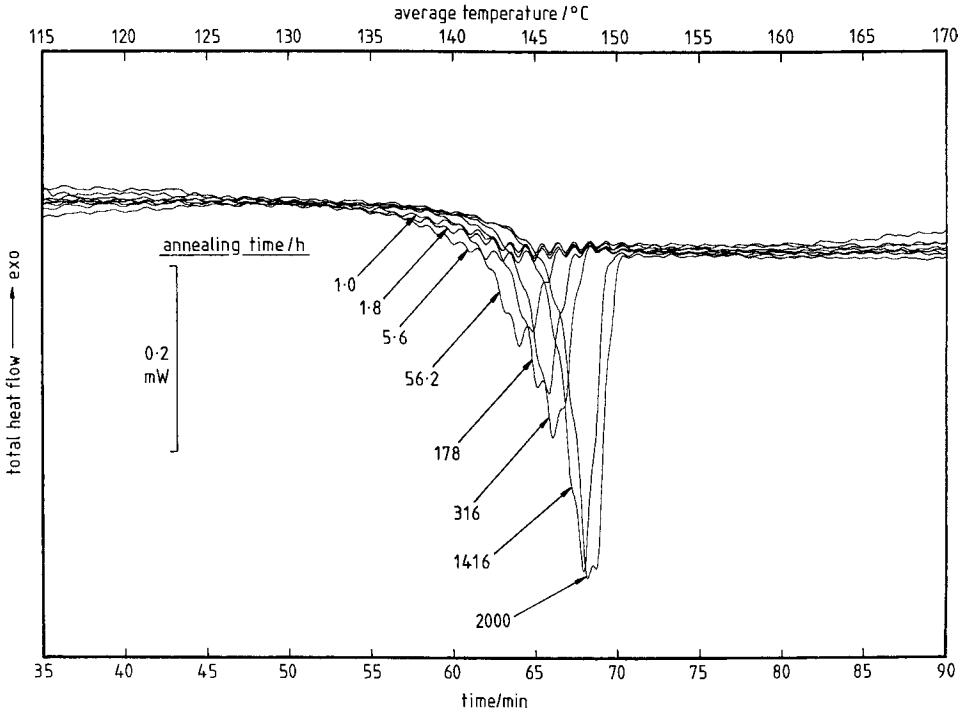

Fig. 4. Total heat flow versus time (lower scale) and temperature (upper scale) for polycarbonate samples annealed at 125°C for the times indicated against each curve. The heat flow scale bar for 0.2 mW is shown, and the exothermic direction is upwards. Note that the temperature scale here, from 115°C to 170°C, is only a part of the full range scanned in the experiments.

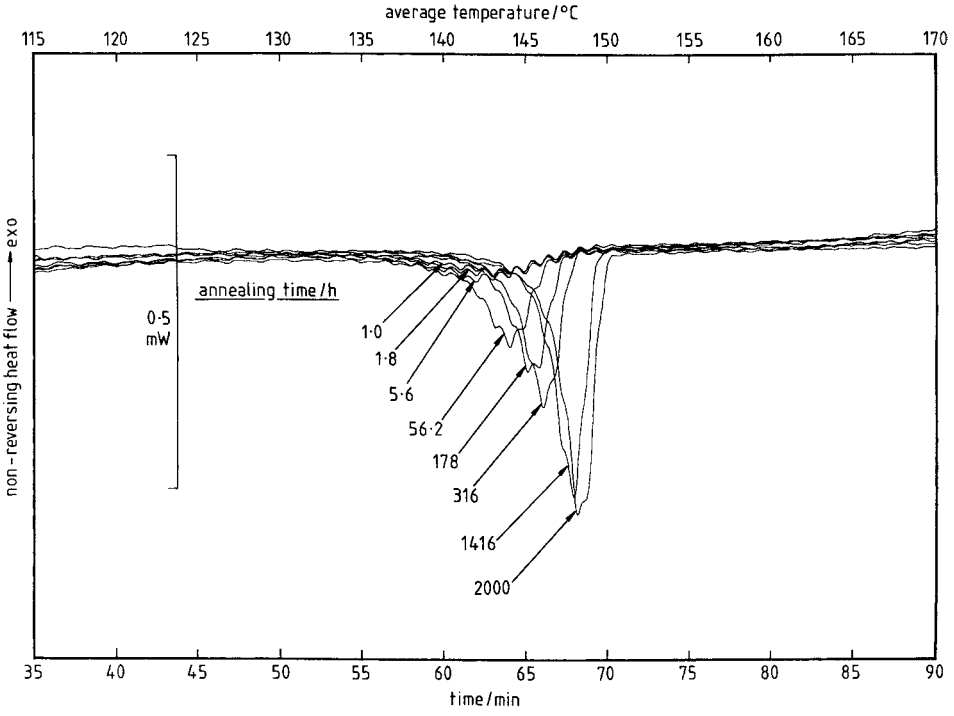

Fig. 5. Non-reversing heat flow versus time (lower scale) and temperature (upper scale) for polycarbonate samples annealed at 125°C for the times indicated against each curve. The exothermic direction is upwards. Note that the temperature scale, from 115°C to 170°C, covers only a part of the full range scanned in the experiments.

the liquid state. Indeed, the non-reversing heat flow should be zero on either side of the transition; this is not shown, however, in Fig. 5 where a relative scale rather than an absolute scale has been used for the heat flow in order to obtain better superposition of the family of curves.

It can also be seen, in both Figs. 4 and 5, that there is a uniform ripple superimposed on the heat flow traces, most noticeably within the transition region. The period of these ripples is the same as the imposed modulation period, and results from the windowing procedure adopted for the Fourier transformation.

The effect of aging on the complex specific heat capacity C_p^* is shown in Fig. 6 for aging times between 0.18 and 562 h. The overall effect is of the transition becoming sharper as the annealing time increases. This sharpening of the transition occurs by virtue of the onset moving towards higher temperatures, whereas the endset remains rather unaffected. The result is therefore that the mid-point temperature T_{mid} shifts towards higher temperatures on aging (see later).

For aging times longer than 562 h, namely for 1416 and 2000 h, the C_p^* traces, which are shown in Fig. 7, became extremely sharp, did not superpose so well on the other traces (Fig. 6), and began to display irregular behaviour, such as the dip in the 2000 h trace which occurs immediately before the sharp increase. These effects may be due to the fact, more clearly visible in the heat flow modulations shown in Fig. 8, that the transition has now become so sharp that it hardly contains six modulation periods, thus throwing some doubt on the validity of the Fourier transformation procedure for these long annealing times. Comparison of Fig. 8 with Fig. 1 also clearly shows the larger endothermic overshoot in the former caused by the enthalpy loss during the long annealing period at 125°C.

The dependence of the corrected phase angle on the aging time is shown in Fig. 9, the correction being made between 136°C and 156°C, and according to the

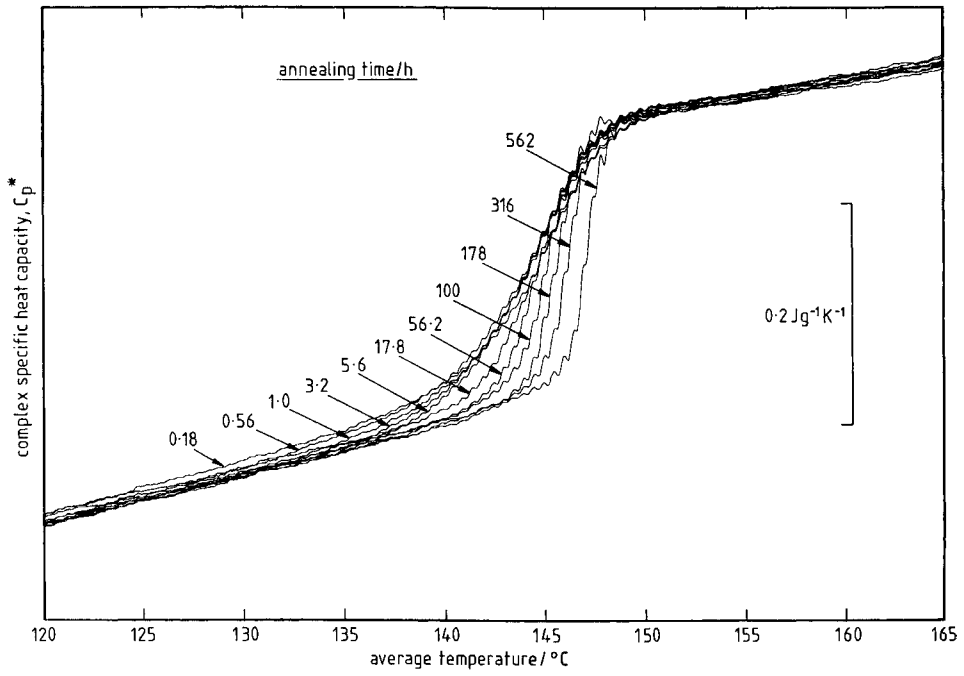

Fig. 6. Complex specific heat capacity as a function of average temperature for polycarbonate samples aged at 125°C for the times indicated against each curve. Note that the temperature scale here, from 120°C to 165°C, is only a part of the full range covered in the experiments.

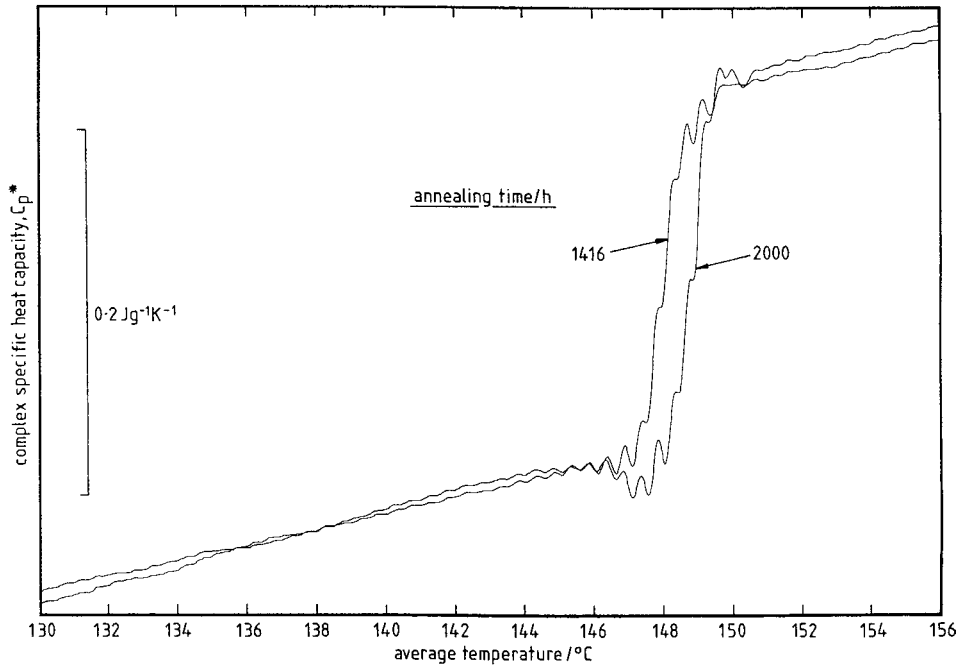

Fig. 7. Complex specific heat capacity traces for annealing times of 1416 and 2000 h. Note the increasingly narrowed temperature range, now from 130°C to 156°C.

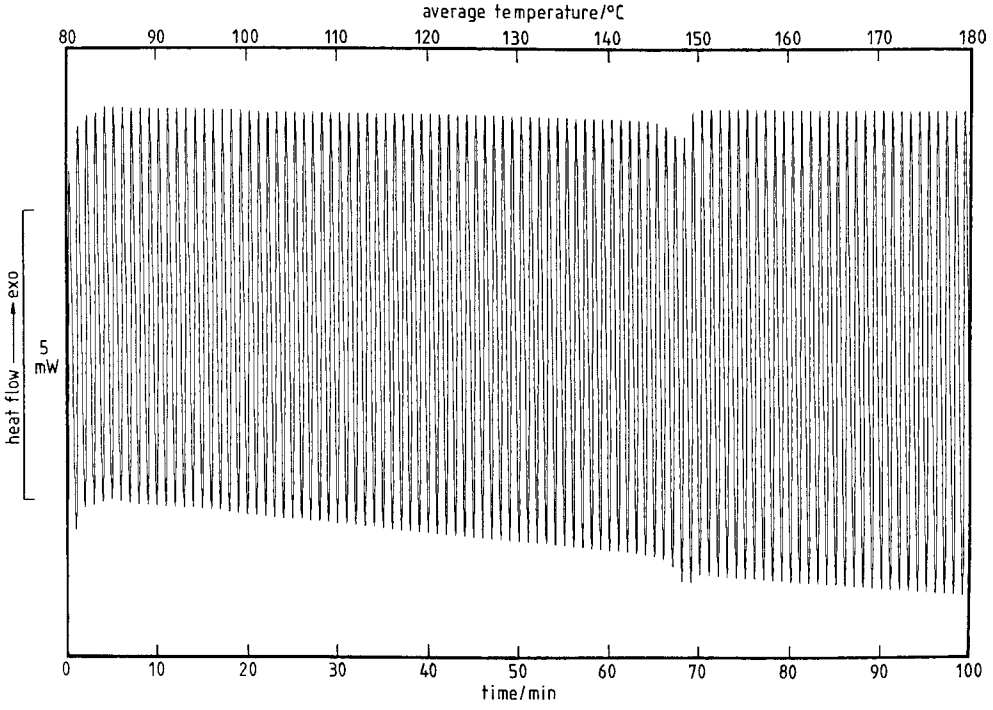

Fig. 8. Heat flow modulations for polycarbonate sample annealed at 125°C for 2000 h and then scanned in the ADSC using a 1,1,1 programme. Exothermic heat flow is upwards, and both time (lower) and average temperature (upper) scales are given.

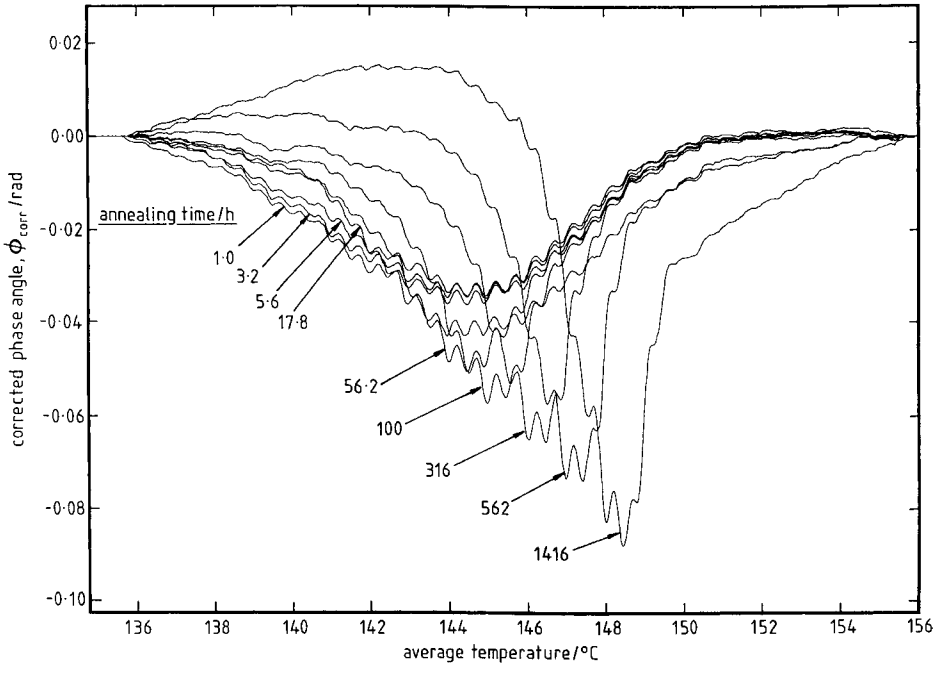

Fig. 9. Corrected phase angle as a function of average temperature for polycarbonate samples annealed at 125°C for the aging times indicated against each curve. The phase angle correction was made between 136°C and 156°C.

procedures described above and in [8–10]. This ensures that the corrected phase angle is zero outside this temperature range, i.e., in the glassy and equilibrium liquid-like states. The overall effect of aging is of a narrowing of the peak, which occurs mainly by virtue of a shift of the low temperature tail towards higher temperatures. This has the simultaneous effect of shifting the temperature of the peak, T_{max} (ϕ), to higher temperatures (see later).

Similar to the heat flow curves in Figs. 4 and 5, the complex specific heat capacity (Figs. 6 and 7) and the corrected phase angle (Fig. 9) also show uniform ripples superimposed on the curves. For these latter, the ripple period is exactly half the imposed modulation period. These ripples, again due to the windowing procedure in the Fourier transformation, have been noted previously [13], and are also present in the theoretical curves [7].

5. Discussion

The numerous curves presented above will now be discussed in the light of theoretical predictions for the ADSC response of aged polymer glasses [7] or in the light of the well-known response in conventional DSC.

Consider first the total heat flow curves of Fig. 4. These are anticipated to be identical to the conventional DSC trace that would obtain at the same underlying heating rate (1 K min^{-1} in the present case). They are certainly very similar in their general aspect, though the ADSC data are distinguished from conventional DSC data in the appearance of the ripples. To make a more quantitative comparison, we can examine the peak temperature T_p at which the total heat flow passes through its endothermic maximum, and this is shown in Fig. 10 where T_p is plotted as a function of the aging time at 125°C, on a logarithmic time scale. This plot, which at first sight seems somewhat strange, can be rationalised as follows.

First it must be recalled that the reheating in conventional DSC of poorly stabilised glasses, that is to say glasses which have been annealed only a little, can give rise to an endothermic peak known as an "upper" peak, which is quite different in nature from the usual annealing or "main" endothermic peak that appears for well annealed samples [14–17]. An upper peak is characterised by a peak temperature which does not vary with annealing time; in contrast, a main peak is

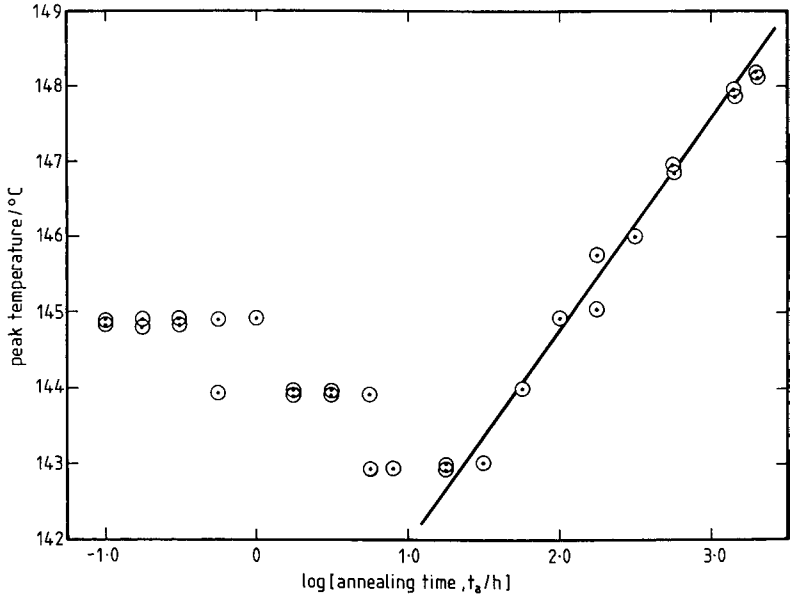

Fig. 10. Peak endothermic temperatures, evaluated from the total heat flow curves such as those shown in Fig. 4, plotted as a function of log (annealing time). The full line is drawn as the least squares fit to the data for annealing times greater than 10 h.

characterised by a peak temperature which increases approximately linear with log (annealing time). The circumstances which favour the appearance of an upper peak are: (i) a heating rate slower than the previous cooling rate, and (ii) only a small amount of annealing.

Since the cooling rate prior to annealing the polycarbonate samples here was 10 K min^{-1} and the underlying heating rate in the ADSC was 1 K min^{-1}, the first of these conditions is met. The second condition is met for short annealing times.

The data in Fig. 10 may therefore be considered as displaying two kinds of peak: an upper peak for short annealing times, and a main annealing peak for long times. The former should be rather constant, but is confused by the appearance of the ripples. The magnitude of these ripples for short annealing times is at least as great as the very small endothermic overshoot that occurs for upper peaks. Furthermore, their period is that of the applied modulations in temperature, namely 1 min, so that for an underlying heating rate of 1 K min^{-1} the upper peak temperature is effectively quantised at 1 K intervals, as is clearly seen in Fig. 10.

For longer annealing times, greater than about 10 h, on the other hand, there is a strong linear dependence of T_p on log (annealing time) as is observed in conventional DSC of polymer glasses. Indeed, the slope of the best fit straight line indicated in Fig. 10 is 2.80 K per decade, closely similar to the value of 2.58 K per decade obtained on the same polycarbonate samples in conventional DSC at a heating rate of 10 K min^{-1} following cooling at 10 K min^{-1} from above T_g and annealing for periods up to 2000 h at 125°C [18]. The effect of the decade difference in heating rates between ADSC and conventional DSC is to shift the peak temperatures for the latter by about 8 K to higher temperature, whilst retaining approximately the same slope.

A further effect of this decade difference in heating rates is to change the annealing time at which the switch from upper peak behaviour (short annealing times) to main peak behaviour (long annealing times) occurs. In conventional DSC at a heating rate of 10 K min^{-1}, this was found to occur at about 1 h [18]. The present ADSC data in Fig. 10 suggest the change occurs at about 10 h when the heating rate is 1 K min^{-1}, in other words an increase of about 1 decade in time for a reduction of 1 decade in heating rate. Qualitatively, at least, this agrees with our expectations: the slower is the heating rate, the longer the glass must be annealed before it appears, for that heating rate, to be well stabilised.

The total heat flow curves of Fig. 4 include, of course, a sigmoidal step change on passing through the glass transition region. When the reversing component of the heat flow is subtracted from this total heat flow, the non-reversing heat flow curves shown in Fig. 5 are obtained. Clearly these do not show any sigmoidal baseline change, and it is tempting, therefore, to consider the area under these non-reversing heat flow curves as a measure of the enthalpy lost during annealing, as has been suggested previously [19]. Allowance must be made, of course, for the fact that during the cooling stage prior to annealing there is also a peak in the non-reversing heat flow. When the area under this cooling peak (1.13 J g^{-1}) is subtracted from the areas under the peaks shown in Fig. 5, the resulting values of "enthalpy loss" as a function of log (annealing time) are shown in Fig. 11. Also shown for comparison are the values of enthalpy loss obtained by conventional DSC at a heating rate of 10 K min^{-1} using the same polycarbonate samples annealed at 125°C in the same way [18].

It can be seen that, for annealing times up to about 300 h, the area difference from the non-reversing heat flow curves is significantly different from that found by conventional DSC. First, it underestimates the enthalpy loss by about 0.5 J g^{-1} for much of the range of annealing times. Second, it overestimates (here by about 10%) the slope of the linear region of the enthalpy loss versus log (annealing time). The same effect can be seen in the aging of polystyrene by comparing the slope of the line in Fig. 4 of [19], the "relaxation enthalpy" versus ln(aging time) from modulated DSC, which gives approximately 1.3 J g^{-1} per decade, with other literature values of approximately 0.8 J g^{-1} per decade (quoted in Table 2 of [12]) for polystyrene aged 15°C below T_g. For annealing times longer than about 300 h, however, the non-reversing heat flow now dramatically overestimates the enthalpy loss, and at a rapidly increasing rate. As a consequence, the non-reversing area difference cannot be considered as an acceptable measure of the enthalpy loss during aging unless a precision of at best 0.5 J g^{-1} is deemed to be satisfactory, and even then is likely to be significantly in error when rather

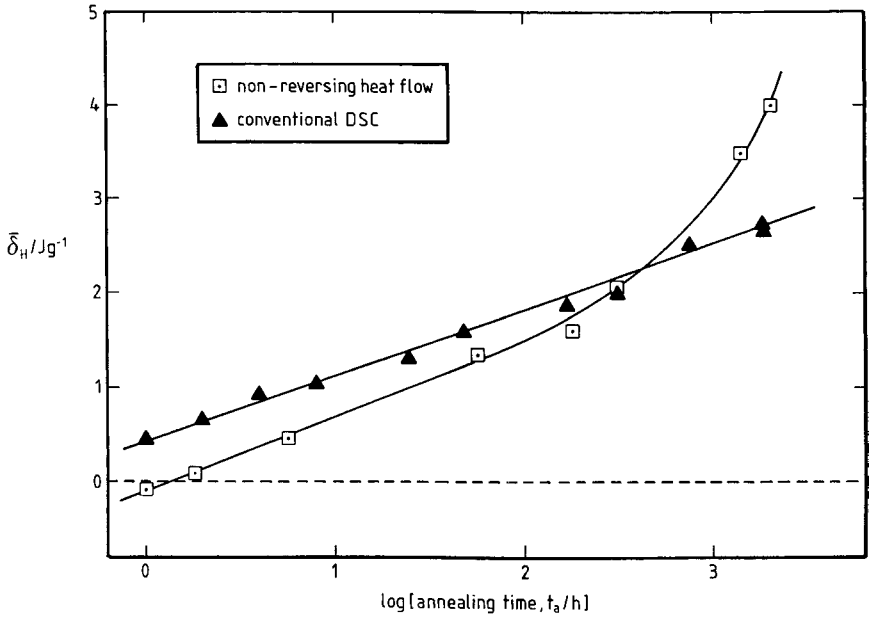

Fig. 11. Area difference between non-reversing heat flow curves in Fig. 5 and heat flow curve on cooling (for the same conditions, i.e., cooling rate=1 K min^{-1}, amplitude=1 K, period=1 mm), plotted as a function of log (annealing time) for samples of polycarbonate annealed at 125°C (open squares). The values of enthalpy loss obtained from conventional DSC on the same polycarbonate samples (see [18]) are shown as filled triangles.

long annealing times are involved. In general, however, an accuracy of better than 0.5 J g^{-1} in the enthalpy loss is required, and is achievable in conventional DSC; hence the latter is to be recommended for any quantitative studies of enthalpy changes due to aging.

The reason for the greater slope in Fig. 11 for the non-reversing heat flow data compared with the conventional DSC data can be found from a consideration of Fig. 6. This shows that the effect of aging is a significant change in the complex specific heat capacity, in other words in the reversing heat flow. Since the reversing heat flow is subtracted from the total heat flow to give the non-reversing heat flow, and the area under the total heat flow curve gives, by definition, the enthalpy loss, the area under the non-reversing heat flow will inevitably be affected by the changes in the reversing heat flow curve during aging. The effect of increased aging is to reduce the area under the reversing heat flow curve, and hence to increase the non-reversing heat flow area relative to the total heat flow area. This can be seen clearly in Fig. 12, where the non-reversing heat flow and total heat flow curves, relative to a reference aging time of 1 h, are both compared with the conventional DSC data, also relative to a reference aging time of 1 h. The total heat flow data agree with the conventional DSC data, albeit with somewhat greater scatter, up to about 300 h aging time, whereas the non-reversing heat flow data display a slightly higher slope. For longer aging times than 300 h, however, it is clear that both sets of ADSC data deviate significantly from the conventional DSC results. The reason for the deviation of the total heat flow possibly lies in the fact that for aging times of more than 1000 h the number of modulations within the dynamic transition region is small, certainly less than 10, and consequently the Fourier transformation procedure may cause a substantial error in the analysis.

Turning now to the complex specific heat analysis, the original data are presented as complex specific heat capacity in Figs. 6 and 7, and as corrected phase angle in Fig. 9, all with families of curves for a range of aging times. From these original curves we may extract the characteristic temperatures T_{mid} and T_{max} (ϕ), the relaxation widths W and $W_{1/2}$, and the phase

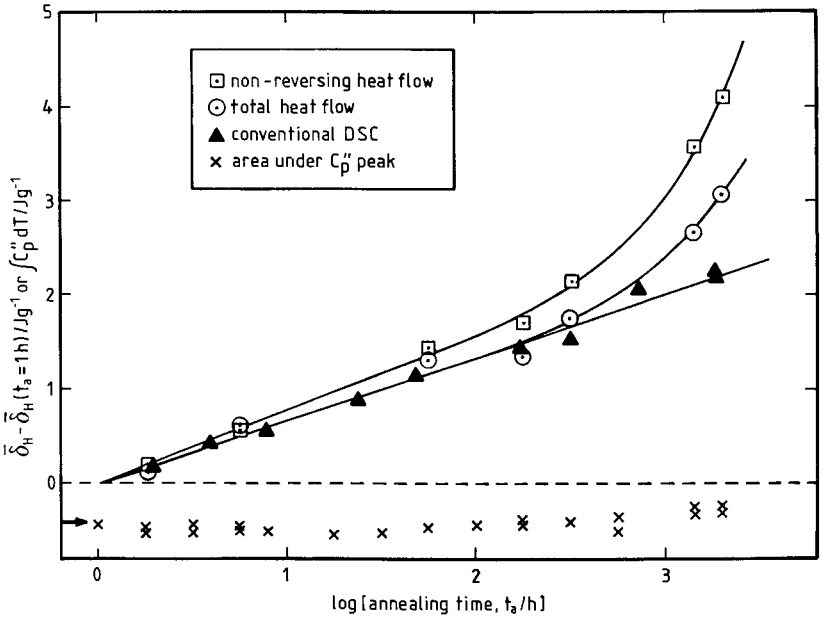

Fig. 12. Depedence on log (annealing time) of the area under the non-reversing heat flow (open squares) and the total heat flow (open circles) curves compared with conventional DSC data (filled triangles), all relative to a reference aging time of t_a=1 h. The area under the C_p'' curves on heating is shown by the crosses, and the arrow indicates the (negative) area under the C_p'' curve on cooling under the same conditions (i.e., cooling rate=1 K min^{-1}, amplitude=1 K, period=1 min).

angle departure from zero, all of which have previously been defined in Fig. 3. The results are shown in Figs. 13–15, respectively. For all of these quantities, the dependence on the aging time is very similar to that displayed earlier by the peak temperature T_p, of the total heat flow curve (Fig. 10); there is a kind of "incubation" period, during which there is little change in any of these quantities, until a "threshold" aging time of the order of 10 h is reached, whereupon the sigmoidal change in C_p^* and the peak in the negative phase angle become much sharper (decreasing widths, Fig. 14) and move to higher temperatures (increasing T_{mid} and T_{max} (ϕ), Fig. 13), and the maximum departure of the phase angle increases (Fig. 15). The general trend beyond t_a=10 h is in agreement with the theoretical predictions [7], the latter also showing that the changes on aging occur principally on the low temperature side of the transition step or peak, with all the curves merging on the high temperature side. The incubation period arises, as was seen earlier for T_p (Fig. 10), from a particular kind of kinetic response on heating that occurs when the heating rate is much slower than the cooling rate, and when insufficient time is allowed for adequate enthalpy relaxation to occur. The upper peaks that were discussed above in the context of T_p all have very similar shapes, and hence so also do the dynamic quantities (C_p^* and ϕ) derived from modulations around this kind of response.

Finally, once the phase angle has been corrected for thermal lag, it is a simple matter to evaluate the out-of-phase specific heat capacity C_p'' from Eq. (3). The curves for C_p'' are very similar to those for ϕ, since ϕ is rather small, and hence are not shown here. The area under the C_p'' peaks has been evaluated, however, between the temperature limits of 136°C and 156°C where the phase angle was corrected to zero, and is shown (as crosses) as a function of log (annealing time) in Fig. 12. The magnitude of the area can be seen to remain rather constant for the full range of annealing times, as was also predicted by the theoretical model [7], thus showing quite unequivocally that the area under the C_p'' peak does not provide any information about the enthalpy lost during aging.

Also shown in Fig. 12, by means of the arrow, is the magnitude of the area under the C_p'' peak on cooling.

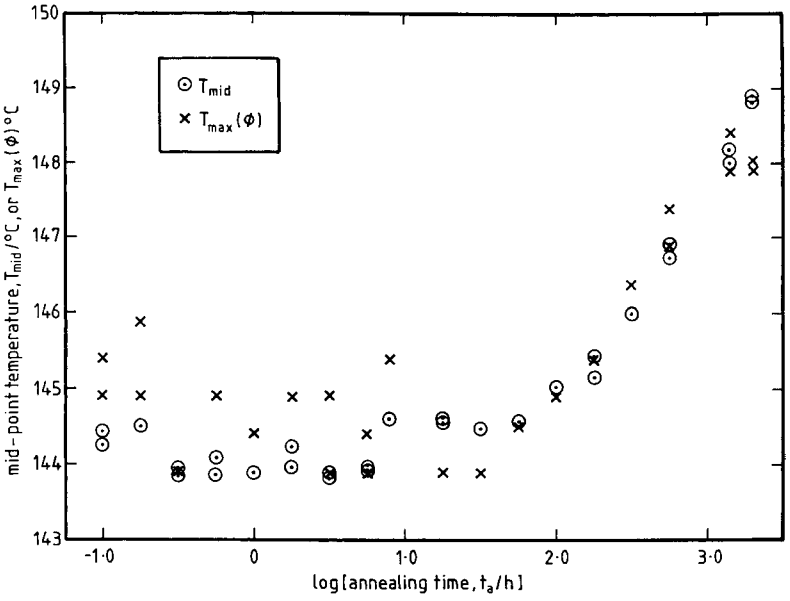

Fig. 13. Mid-point temperature T_{mid} for complex specific heat capacity (open circles) and temperature T_{max} (ϕ) of maximum departure of corrected phase angle (crosses) as a function of log (annealing time) for polycarbonate samples annealed at 125°C.

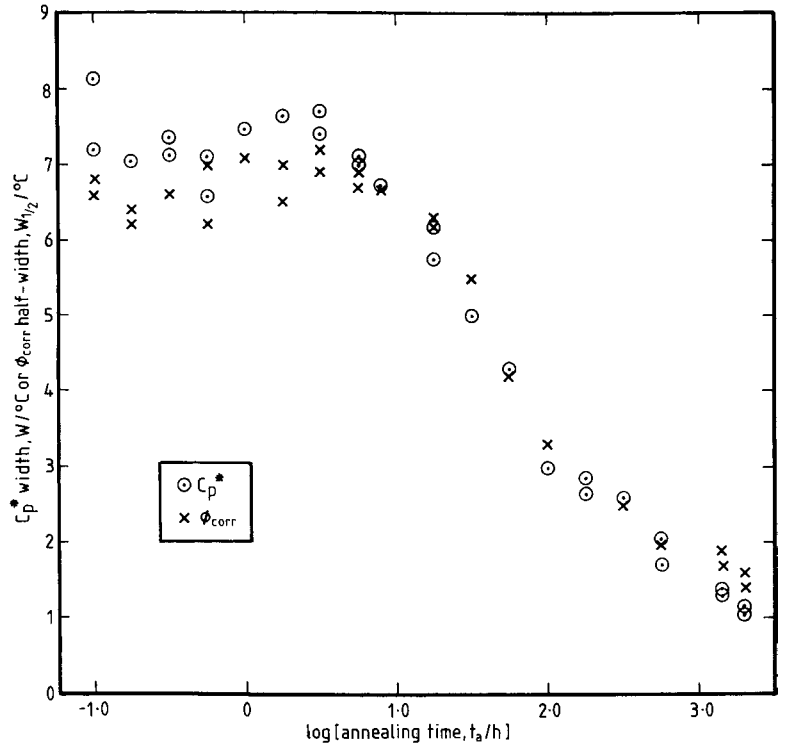

Fig. 14. Width W of C_p^* traces (open circles) and half-width $W_{1/2}$ of corrected phase angle curves (crosses) as a function of log (annealing time) for polycarbonate samples annealed at 125°C.

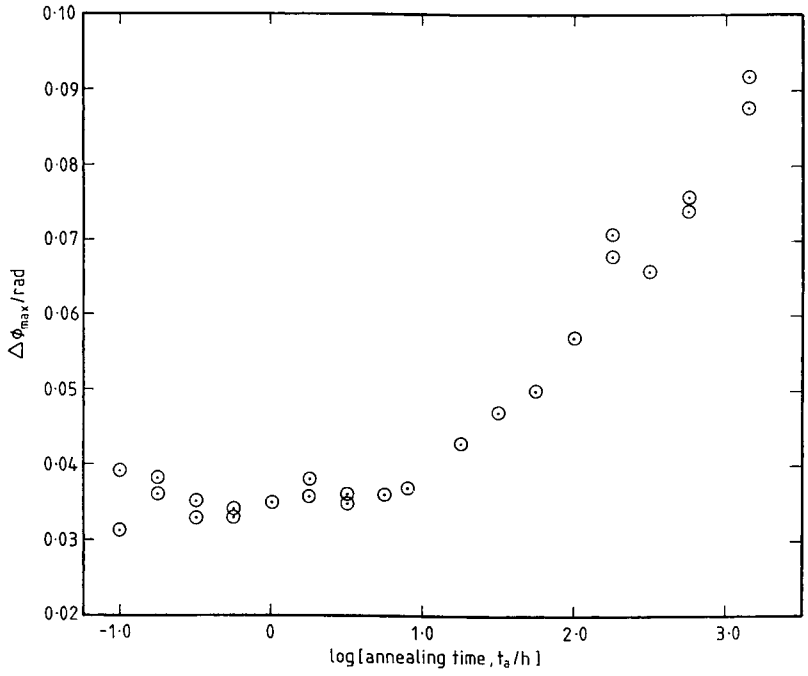

Fig. 15. Maximum departure of corrected phase angle (considered as a positive value) as a function of log (annealing time) for polycarbonate samples annealed at 125°C.

Since the phase angle is negative during heating, the value of C_p'', and hence also the area under the C_p'' peak, is negative during heating, as indicated in Fig. 12. On cooling, both ϕ and C_p'' are again negative, but the area under the peak will be positive since dT/dt is negative. The arrow in Fig. 12 is used, however, at negative values in order to provide an easy comparison of the magnitude of the area on cooling (0.40 J g^{-1}) with those obtained on heating. It can be seen that, within the limits of experimental error in these measurements, there is no clearly significant difference in this area on cooling or on heating. It has not been possible, therefore, to substantiate the anticipated positive value of the circular integral of C_p'' over the whole cooling, annealing, and reheating thermal cycle [7]. It should be pointed out, though, that the magnitude of this circular integral for the theoretical single relaxation time model [7] was only of the order of 0.1 or 0.2 J g^{-1}, which is of the same order as the uncertainty in the experimental values, given the substantial amount of data treatment, including the phase angle correction, involved in this process.

6. Conclusions

The effect of annealing polycarbonate at 125°C, 20 K below its glass transition temperature, has been studied by ADSC using a 1,1,1 temperature programme. It is shown that the response of annealed samples can be described by a number of features which are in good agreement with the prediction of an earlier theoretical model [7], and which can be summarised as follows.

1. The total heat flow closely resembles the response of conventional DSC in respect of the endothermic peak temperature and the enthalpy loss (derived from the area under the peak). The precision of the ADSC response, however, is less than that of conventional DSC because of the appearance of ripples in the ADSC trace.
2. The area under the non-reversing heat flow peak cannot be considered as a good approximation to the enthalpy loss on aging, particularly for long aging times.

3. The complex specific heat capacity (and the reversing heat flow) shows a sigmoidal change at the glass transition, which becomes sharper as the annealing time increases. This occurs almost entirely by a shift of the low temperature tail of the relaxation towards higher temperatures, with the result that the mid-point of the transition, T_{mid}, moves to higher temperatures on aging.
4. Similarly, the corrected phase angle becomes sharper and its (negative) peak moves towards higher temperatures as the aging time increases.
5. The area under the out-of-phase specific heat capacity peak remains essentially constant as a function of aging time, confirming that it provides no information about the enthalpy loss that occurs during the aging process.

Acknowledgements

We are grateful to Mettler-Toledo for financial support for this project.

References

[1] M. Reading, Trends in Polym. Sci. 1 (1993) 248.
[2] J.C. Seferis, I.M. Salin, P.S. Gill, M. Reading, Proc. Acad. Greece 67 (1992) 311.
[3] G. Van Assche, A. van Hemelrijck, H. Rahier, B. van Mele, Thermochim. Acta 268 (1995) 121.
[4] S. Montserrat, I. Cima, Thermochim. Acta 330 (1999) 189.
[5] J.M. Hutchinson, S. Montserrat, J. Therm. Anal. 47 (1996) 103.
[6] J.M. Hutchinson, S. Montserrat, Thermochim. Acta 286 (1996) 263.
[7] J.M. Hutchinson, S. Montserrat, Thermochim. Acta 304 305 (1997) 257.
[8] S. Weyer, A. Hensel, C. Schick, Thermochim. Acta 304 305 (1997) 267.
[9] Z. Jiang, C.T. Imrie, J.M. Hutchinson, Thermochim. Acta 315 (1998) 1.
[10] C.T. Imrie, Z. Jiang, J.M. Hutchinson, Mettler-Toledo User Com. 6 (1997) 20.
[11] I.M. Hodge, J. Non-Cryst. Solids 169 (1994) 211.
[12] J.M. Hutchinson, Prog. Polym. Sci. 20 (1995) 703.
[13] J.M. Hutchinson, C.T. Imrie, Z. Jiang, Mettler-Toledo User Com. 6 (1996) 22.
[14] J.M. Hutchinson, A.J. Kovacs, Polym. Eng. Sci. 24 (1984) 1087.
[15] J.M. Huchinson, M. Ruddy, J. Polym. Sci., Polym. Phys. Edn. 26 (1988) 2341.
[16] J.M. Hutchinson, M. Ruddy, J. Polym. Sci., Polym. Phys. Edn. 28 (1990) 2127.
[17] J.M. Hutchinson, Progr. Colloid Polym. Sci. 87 (1992) 69.
[18] J.M. Hutchinson, S. Smith, B. Horne, G.M. Gourlay, Macromolecules 32 (1999) 5046.
[19] D.J. Hourston, M. Song, A. Hammiche, H.M. Pollock, M. Reading, Polymer 37 (1996) 243.